



Published in final edited form as:

J Bone Miner Res. 2015 June ; 30(6): 1064–1076. doi:10.1002/jbmr.2433.

Gender-Specific Differences in the Skeletal Response to Continuous PTH in Mice Lacking the IGF1 Receptor in Mature Osteoblasts

Muriel Babey, Yongmei Wang, Takuo Kubota, Chak Fong, Alicia Menendez, Hashem Z ElAlieh, Daniel D Bikle

Endocrine Research Unit, University of California, San Francisco, CA, USA

Abstract

The primary goal of this study was to determine whether the IGF1R in mature osteoblasts and osteocytes was required for the catabolic actions of continuous parathyroid hormone (cPTH). *Igfr1* was deleted from male and female FVN/B mice by breeding with mice expressing cre recombinase under control of the osteocalcin promoter (*OCN-Igfr1^{-/-}*). Littermates lacking the cre recombinase served as controls. PTH, 60 µg/kg/d, was administered continuously by Alzet minipumps for 4 weeks. Blood was obtained for indices of calcium metabolism. The femurs were examined by micro-computed tomography for structure, immunohistochemistry for IGF1R expression, histomorphometry for bone formation rates (BFR), mRNA levels by qPCR, and bone marrow stromal cell cultures (BMSC) for alkaline phosphatase activity (ALP⁺), mineralization, and osteoblast-induced osteoclastogenesis. Whereas cPTH led to a reduction in trabecular bone volume/tissue volume (BV/TV) and cortical thickness in the control females, no change was found in the control males. Although trabecular BV/TV and cortical thickness were reduced in the *OCN-Igfr1^{-/-}* mice of both sexes, no further reduction after cPTH was found in the females, unlike the reduction in males. BFR was stimulated by cPTH in the controls but blocked by *Igfr1* deletion in the females. The *OCN-Igfr1^{-/-}* male mice showed a partial response. ALP⁺ and mineralized colony formation were higher in BMSC from control males than from control females. These markers were increased by cPTH in both sexes, but BMSC from male *OCN-Igfr1^{-/-}* also were increased by cPTH, unlike those from female *OCN-Igfr1^{-/-}*. cPTH stimulated receptor activator of NF-κB ligand (RANKL) and decreased osteoprotegerin and alkaline phosphatase expression more in control female bone than in control male bone. Deletion of *Igfr1* blocked these effects of cPTH in the female but not in the male. However, PTH stimulation of osteoblast-driven osteoclastogenesis was blocked by deleting *Igfr1* in both sexes. We conclude that cPTH is catabolic in female but not male mice. Moreover, IGF1 signaling plays a greater role in the skeletal actions of cPTH in the female mouse than in the male mouse, which may underlie the sex differences in the response to cPTH.

Address correspondence to: Muriel Babey, MD, and Daniel Bikle, MD, PhD, Endocrine Research Unit, UCSF, 111N-MB, 1700 Owens Street, San Francisco, CA 94158, USA., muriel.babey@gmail.com; daniel.bikle@ucsf.edu.

Disclosures

All authors state that they have no conflicts of interest.

Additional Supporting Information may be found in the online version of this article.

Keywords

IGF1 RECEPTOR; MATURE OSTEOBLAST; CONTINUOUS PTH; SEX DIFFERENCE; OSTEOCLAST

Introduction

Primary hyperparathyroidism is a common disease with a prevalence of 2.1% in postmenopausal females.⁽¹⁾ For reasons not readily apparent, the disease is more common in females.⁽²⁾ Parathyroid hormone (PTH) stimulates both bone formation and resorption by increasing the number and/or activity of osteoblasts, osteocytes, and osteoclasts.^(3–5) The balance between bone formation and resorption is dependent on the pharmacodynamics of administration. When given intermittently, PTH (iPTH) is anabolic for most skeletal sites.^(6–8) This has led to approval of iPTH for the treatment of osteoporosis. The increase in bone formation is attributable primarily to increased osteoblast number as a result of increased proliferation and differentiation of osteoblasts^(9,10) in part owing to inhibition of SOST expression in osteocytes with promotion of wnt signaling,⁽¹¹⁾ as well as increased IGF1 expression,^(12–14) decreased osteoblast apoptosis,⁽¹⁵⁾ and activation of bone lining cells.⁽¹⁶⁾ Continuous exposure to PTH (cPTH) as in primary hyperparathyroidism is generally catabolic because its stimulation of bone resorption exceeds that of its stimulation of bone formation.^(17,18) PTH stimulates bone resorption in part by induction of receptor activator of NF- κ B ligand (RANKL) and suppression of osteoprotegerin (OPG) by osteoblasts and osteocytes, resulting in the differentiation and subsequent activation of osteoclast precursors.⁽¹⁷⁾ The mature osteoblast and osteocyte⁽¹⁹⁾ are important targets for these actions of PTH in that the receptor for PTH (PTHR) increases with differentiation (maturation) of the osteoblast, and the ability of PTH to induce RANKL and osteoclastogenesis parallels PTHR expression.⁽²⁰⁾ Moreover, cPTH has been reported to decrease IGF1 expression compared with iPTH,⁽²¹⁾ thus reducing the anabolic actions mediated by this growth factor.

IGF1 stimulates osteoprogenitor proliferation and differentiation⁽²²⁾ as well as osteoclast formation in vitro.⁽²³⁾ Mice lacking IGF1 production globally (*Igf1*^{-/-}) are deficient in both bone formation and bone resorption with few osteoblasts or osteoclasts in bone in vivo, reduced osteoblast colony-forming units, and an inability of either the osteoblasts or osteoclast precursors to support osteoclastogenesis in vitro.^(23,24) Mice in which the IGF1 receptor (*Igfr1*) is specifically deleted in mature osteoblasts (*OCN**Igfr1*^{-/-}) using an osteocalcin-driven cre recombinase have a mineralization defect in vivo,⁽²⁵⁾ and bone marrow stromal cells (BMSC) from these mice fail to mineralize in vitro.⁽²⁶⁾ iPTH fails to stimulate bone formation in the *Igf1*^{-/-} or *OCN**Igfr1*^{-/-} mouse. The question we are asking in this study is whether *OCN**Igfr1*^{-/-} mice also lack the ability to respond to cPTH with respect to increased skeletal catabolism. Because of the sex differences in humans with respect to prevalence of primary hyperparathyroidism and our recent observations that female mice have a greater catabolic response in a model of primary hyperparathyroidism,⁽²⁷⁾ we evaluated the response to cPTH in both sexes of the *OCN**Igfr1*^{-/-} mice. As expected, cPTH promotes a catabolic skeletal response in the female mice, and this is blocked in mice lacking IGF1R in their mature osteoblasts and osteocytes. To our surprise, the response in

the male mice is on balance anabolic, with at least partial preservation of this anabolic effect even in the *OCN^{Cre}Igfr1^{-/-}* mouse, suggesting that the role of IGF1 signaling in the skeletal actions of PTH is sex specific.

Materials and Methods

Mice

Homozygous conditional mice in which exon 3 of the *Igfr1* gene was flanked by loxP sites were bred with heterozygous mice in which cre recombinase was expressed under the control of the human osteocalcin promoter (gift from Dr Thomas Clemens) to generate mature osteoblast and osteocyte-specific *Igfr1*-deficient mice. The mice were maintained under pathogen-free conditions, fed *ad libitum*, and exposed to a 12:12-hour light-dark cycle. Animal protocols were approved by the Institutional Animal Care and Use Committee at the Veterans Administration Medical Center, San Francisco.

Immunohistochemistry

Following our previously reported methods,⁽²⁸⁾ femurs were cleaned of adherent tissue, fixed overnight at 4 °C in 4% paraformaldehyde in PBS, rinsed in PBS, dehydrated through an ethanol series, cleared in xylene, embedded in paraffin, and cut into 5- μ m sections. Deparaffinized and rehydrated sections were incubated with 3% hydrogen peroxide in methanol to block endogenous peroxidase and with protein blocker (Abcam, Cambridge, MA, USA) to block the nonspecific binding of antibodies. The sections were then reacted with rabbit IGF1R antibody (1:200) (Aviva Systems Biology, San Diego, CA, USA) at 4 °C overnight. After washing with PBS, the sections were incubated with biotinylated goat anti-rabbit IgG (Abcam), then streptavidin peroxidase (Abcam), and visualized by 3,3'-diaminobenzidine.

Continuous PTH infusion

We infused 12-week-old female and male mice with continuous rat PTH 1–34 (Bachem, Torrance, CA, USA) at a dose of 60 μ g/kg body weight or vehicle solution via ALZET mini osmotic pumps (Model 1004) over a period of 4 weeks. The PTH was reconstituted in the vehicle solution containing 150 mM NaCl, 1 mM HCl, and 2% heat-inactivated mouse serum. The mini osmotic pumps were implanted into an interscapular subcutaneous pocket under Avertin anesthesia. There were at least 8 mice in each group.

Serum biochemistry

Blood samples were drawn by cardiac puncture during euthanasia by isoflurane inhalation and allowed to clot in BD Microtainer Tubes (#365956, BD, Franklin Lakes, NJ, USA). The samples were then centrifuged and the serum analyzed for total serum Ca²⁺ (sCa), inorganic phosphate (sPi), and alkaline phosphatase (sALP) by an automated ACE Alera Clinical Chemistry bioanalyzer (Alfa Wassermann, Inc., West Caldwell, NJ, USA) as we have previously reported.⁽²⁷⁾ Serum intact PTH (sPTH) and IGF1 concentrations were assessed using commercial ELISA kits made by Immotopics (San Clemente, CA, USA) as previously reported.⁽²⁷⁾

Measurement of bone mineral content and structure by micro-computed tomography (μ CT)

Femurs for in vitro μ CT analysis were isolated, fixed in 10% phosphate-buffered formaldehyde (PBF) for 24 hours, and maintained in 70% ethanol. Trabecular and cortical bone sections were scanned by a Scanco vivaCT 40 scanner (Scanco Medical AG, Bruttisellen, Switzerland) with 10.5- μ m voxel size and 55-kV X-ray energy. For trabecular bone, 100 serial crosssectional scans (1.05 mm) of the secondary spongiosa of the left distal femoral metaphysis were obtained from the end of the growth plate extending proximally to the shaft. For cortical bone, 100 serial cross sections (1.05 mm) of the femoral midshaft were scanned. The voxel had an isotropic size of 21 μ m and X-ray energy 55 kV. A threshold of 420 mg hydroxyapatite (HA)/mm³ was applied to segment total mineralized bone matrix from soft tissue. Linear attenuation was calibrated using hydroxyapatite phantom. To assess bone mineral density (BMD) by mCT, X-ray attenuation in the volume of interest (including both bone and non-bone voxels) in cancellous bone was measured and reported in units of hydroxyapatite density (mgHA/ccm) or HU. μ CT image analysis and 3D reconstructions were performed using software provided by Scanco. Data were reported according to standard μ CT nomenclature. These methods are standard in our laboratory and follow published guidelines.⁽²⁹⁾

Bone marrow stromal cell culture

The left tibial and femoral bone marrow stromal cells were harvested using techniques previously described.⁽²²⁾ The tibias and femurs were collected and the soft tissue was removed. The epiphyses of each bone were removed, and the bone marrow was flushed from the diaphysis with a syringe and a 26-gauge needle. The marrow from each individual mouse was collected in primary culture medium (alpha modification of Eagle's medium [α -MEM] containing L-glutamine and nucleosides; Mediatech, Herndon, VA, USA), supplemented with 10% fetal bovine serum (FBS; Atlanta Biologicals, Norcross, GA, USA), 100 U/mL penicillin/streptomycin (Mediatech), 0.25 μ g/mL fungizone (Life Technologies, Grand Island, NY, USA). A single-cell suspension was obtained by repeated passage through an 18-gauge needle. A pool of BMSCs was made from the tibia and femur of each mouse. The cells were plated at 2×10^6 cells/well in 6-well plates. Nonadherent cells were removed by aspiration, and then the primary medium was replenished on day 5. On day 7, the cells were provided with secondary medium (the primary medium with 3 mM β -glycerophosphate and 50 μ g/mL ascorbic acid; Sigma-Aldrich, St. Louis, MO, USA). Subsequent medium changes were performed every 2 days for up to 21 days. At day 14 of culture, cells were assessed using SIGMAFAST BCIP/NBT tablet (Sigma cat. no. B5655) to determine alkaline phosphatase (ALP)⁺ colony-forming units (CFUs) following the manufacturer's instructions. At day 21 of culture, calcium nodules were stained with silver nitrate for 10 minutes, the stain was aspirated, and the dishes were rinsed five times by distilled water to remove loosely bound stain. Stained cultures were scanned and quantified using Improvision Openlab software version 5.0.2.

Histomorphometry

To obtain trabecular bone formation measurements, demeclocycline (30 mg/kg, Sigma-Aldrich) and calcein (15 mg/kg, Sigma-Aldrich) were given peritoneally to mice 7 days

and 2 days before euthanasia, respectively. Femurs were fixed, dehydrated, and embedded in methyl methacrylate. Cross-sectional undecalcified sections (10 μm) from the secondary spongiosa of the distal femur metaphysis were cut to assess bone formation in trabecular bone. Mosaic-tiled images were converted to a single image by the Axio Vision software (Carl Zeiss, Thornwood, NY, USA). Data were collected using the Bioquant Osteo software (Bioquant Image Analysis, Nashville, TN, USA) and reported according to standard bone histomorphometry nomenclature. Bone formation rate/bone surface (BFR/BS) ($\mu\text{m}^3/\mu\text{m}^2/\text{d}$) is calculated as the multiplication of mineralizing surface MS/BS and mineral apposition rate (MAR). MS is bone surface actively mineralized by osteoblasts at a particular time when fluorescent labels are administered and calculated as the total extent of double-labeled bone surfaces plus the half of single-labeled bone surfaces. It correlates with the extent of bone surface covered with osteoblasts. MAR is the distance between two labels divided by the time between two labeling periods. These methods are standard in our laboratory⁽²⁶⁾ and follow published guidelines.⁽³⁰⁾

Co-culture of hematopoietic cells and osteoblasts

To study the effects of continuous PTH on co-cultures, the source of osteoblasts came from mice that were infused with cPTH or vehicle solution. Bone marrow stromal cells from 16-week-old *OCN**Igf1r*^{-/-} and control mice were flushed out with a syringe and 26-gauge needle and collected in primary culture medium as a source of osteoblasts. The marrow cell suspension was gently drawn through an 18-gauge needle to mechanically dissociate the mixture into a uniform single cell suspension and then cultured in T-75 flasks at a density of 100×10^6 cells/flask. When the cultures reached 50% to 60% confluence, the cells (stromal/osteoblastic cells) were harvested by $1 \times$ trypsin-EDTA (0.05% trypsin, 0.53 mM EDTA; Cellgro, Mediatech), replated at 20,000 cells/well in 24-well plates ($n = 3-6$ wells), and incubated in primary medium supplemented with ascorbic acid 50 $\mu\text{g}/\text{mL}$ (secondary medium) for 4 or more days, with media changes every 2 days. As a source of osteoclast precursors, bone marrow cells from 16-week-old control mice were harvested and cultured in α -MEM (Mediatech), supplemented with 10% heat-inactivated FBS (Atlanta Biologicals, Norcross, GA, USA), 100 U/mL penicillin/streptomycin (Mediatech), and 0.25 $\mu\text{g}/\text{mL}$ fungizone (Life Technologies; primary medium) overnight. Nonadherent osteoclast precursors were added (1×10^6 cells/well) to the stromal/osteoblastic cell cultures to create stromal/osteoblastic cell-osteoclast precursor cell co-cultures. The co-cultures were carried for 7 days in secondary media, with media changes every 2 days. On day 7 of the co-culture, the cells were rinsed with PBS and prepared for TRAP staining. These methods are standard in our laboratory.⁽²³⁾

Hematopoietic osteoclast precursor culture

The osteoclast precursors from 16-week-old *OCN**Igf1r*^{-/-} and control mice were prepared as above, transferred to 24-well plates (5×10^5 /well) and cultured with RANKL 30 ng/mL (Sigma) and 10 ng/mL M-CSF (Sigma) for an additional 7 days, with addition of fresh media every 3 days. TRAP staining was performed using a commercial kit (387 A; Sigma).⁽²³⁾

mRNA levels in bone

Femurs and tibias were cleaned of adherent tissue, the marrow flushed out with PBS using a 26-gauge needle, and the bones frozen in liquid nitrogen and stored at -80°C until processed. The bones from each animal were pooled, and bone pools were pulverized in a steel mortar and pestle cooled in liquid nitrogen. RNAs were isolated by an RNA Stat-60 kit (Tel-Test, Friendswood, TX, USA). For each pool, 2000 ng of total RNA was reverse-transcribed in 100 μL of a reaction mixture that contained 10 mM Tris-HCl (pH 8.3), 50 mM KCl, 7.5 mM MgCl_2 , 1 mM of each deoxynucleoside triphosphate, 5 μM of random primers (Gibco, Life Technologies), 0.4 U/ μL of RNase inhibitor (Roche, Mannheim, Germany), and 2.5 U/ μL of Moloney murine leukemia virus reverse transcriptase (Gibco, Life Technologies) at 25°C for 10 minutes, 48°C for 40 minutes, 95°C for 5 minutes, and then stored at 4°C . These methods and the sequences of the PCR primers and probes have been previously reported.^(23,26,31) These primers and probes were designed using Primer Express software (Applied Biosystems, Carlsbad, CA, USA). Primers were synthesized by the Biomolecular Resource Center (University of California, San Francisco, CA, USA). Probes were synthesized by Integrated DNA Technologies, Inc. (Coralville, IA, USA). PCR was carried out in triplicate with 20- μL reaction volumes of 1X TaqMan Universal PCR Master Mix (Applied Biosystems), 500 nM of each primer, 200 nM of probe, and 1 μL of cDNA template. The PCR reaction was performed in an ABI Prism 7900HT sequence detection system using the following cycles: 95°C for 12 minutes, then 40 cycles of 95°C for 15 seconds and 60°C for 1 minute. Analysis was carried out using the sequence detection software supplied with the ABI Prism 7900HT sequence detection system. The Ct values were determined for three test reactions in each sample and averaged. The Ct values were obtained by subtracting the L19 (as endogenous control) Ct values from the target gene Ct values of the same samples. The relative quantification of the target genes was given by $2^{-\text{Ct}}$.

Statistics

Results are given as means \pm standard errors of the mean or standard deviations as indicated in the figure legends. Statistical analyses were performed using unpaired, two-tailed Student's *t* test for comparison between two groups and one-way ANOVA test for comparison of more than two groups using Prism 5. A *p* value <0.05 was considered statistically significant.

Results

Deletion of *Igf1r* in mature osteoblasts and osteocytes in *OCN**Igf1r*^{-/-} mice

To verify that mature osteoblasts and osteocytes were targeted in *OCN**Igf1r*^{-/-} mice, we assessed the expression of *Igf1r* in trabecular bone and cortical bone by IGF1R immunohistochemistry (Supplemental Fig. S1). {FIGS1} *OCN**Igf1r*^{-/-} mice expressed IGF1R in fewer cells in the osteoblast lineage (13% of total cells compared with 50% in controls, with a greater difference in osteocytes) (Fig. 1B, D) {FIG1} compared with control mice (Fig. 1A, C). These results demonstrate the specific deletion of *Igf1r* in mature osteoblasts and osteocytes in *OCN**Igf1r*^{-/-} mice.

Impact of *Igf1r* deletion in mature osteoblasts and osteocytes on bone histomorphometry

Histomorphometry of the distal femur of the 3-month *OCN**Igf1r*^{-/-} mice and their control littermates was performed. The results are shown in Supplemental Fig. S2. {FIG S2} BV/TV was substantially lower in the *OCN**Igf1r*^{-/-} mice in both sexes, with the differences more striking in the female mice. No significant differences were observed in osteoblast numbers/BS, but the osteoclast numbers/BS were significantly reduced in the male *OCN**Igf1r*^{-/-} mice compared with controls and to the female control and *OCN**Igf1r*^{-/-} mice. Both male and female *OCN**Igf1r*^{-/-} mice had decreased BFR/BS compared with littermate controls because of both a reduction in MS/BS and MAR.

Suppressed endogenous intact PTH concentrations in continuously PTH-infused *OCN**Igf1r*^{-/-} and control mice

To confirm that the continuous infusion of rat PTH 1–34 (cPTH) impacted bone metabolism and ultimately PTH secretion in the parathyroid gland, we measured endogenous intact PTH concentrations in all groups after 4 weeks of cPTH. All cPTH mice showed a marked suppression of endogenous intact PTH concentrations (Fig. 1A). No significant differences in endogenous intact PTH concentrations could be found between vehicle-infused control and *OCN**Igf1r*^{-/-} mice for either sex.

Sex and genotype differences in the effect of PTH infusion on serum calcium, alkaline phosphatase, and IGF1 concentrations

cPTH significantly increased the calcium concentrations in the female control mice, but the effect was not present in the female *OCN**Igf1r*^{-/-} mice (Fig. 1B), although total calcium concentrations were significantly higher in vehicle-infused female *OCN**Igf1r*^{-/-} mice compared with female control mice. cPTH had no significant impact on serum calcium in either male controls or *OCN**Igf1r*^{-/-} mice. The serum phosphate concentrations were not significantly affected by genotype, sex, or PTH infusion (data not shown).

ALP activity like serum calcium was significantly increased in cPTH female control mice compared with vehicle-infused control mice (Fig. 1C), and as for serum calcium, this effect was not found in the *OCN**Igf1r*^{-/-} females. The male groups responded differently. There was no increase in ALP activity upon PTH infusion in the male control mice compared with the vehicle-infused control mice. However, ALP activity was significantly reduced in male vehicle-infused *OCN**Igf1r*^{-/-} mice compared with control mice and was markedly elevated in PTH-infused male *OCN**Igf1r*^{-/-} mice, indicating at least a partial effect of PTH in those mice. Thus, sex in addition to genotype clearly affects the response to PTH in both control and *OCN**Igf1r*^{-/-} mice.

Circulating IGF1 is mainly derived from secretion by the liver and largely regulated by growth hormone secreted by the pituitary gland. We anticipated that the knockout of *Igf1r* in mature osteoblasts and osteocytes would not affect IGF1 serum concentrations. However, cPTH male control mice demonstrated a significant increase in IGF1 concentrations compared with vehicle-infused male control mice (Fig. 1D).

Sex and genotype differences in the effect of PTH infusion on trabecular bone

cPTH is expected to produce a primarily catabolic effect on bone, although trabecular bone may be relatively spared.⁽³²⁾ We wanted to know whether these catabolic actions of PTH were dependent on IGF1 signaling. We used high-resolution microtomography (mCT) analysis to examine the trabecular bone architecture in the secondary spongiosa of the distal femur upon vehicle and PTH infusion in all groups. Although the size of the bone was comparable between control and *OCN**Igf1r*^{-/-} mice (males larger than females in both cases) (Fig. 2A, B), {FIG2} bone volume and thus bone volume/tissue volume (BV/TV) was markedly reduced in the *OCN**Igf1r*^{-/-} mice compared with controls of either sex (Fig. 2A, B). Upon PTH infusion, female controls exhibited severe bone loss, which is visualized in a representative 3D reconstruction of that bone region (Fig. 2A). However, the catabolic effects on BV/TV were abolished in female *OCN**Igf1r*^{-/-} mice (Fig. 2A, B). The male control mice showed no net change in trabecular bone architecture after PTH infusion. However, PTH infusion in male *OCN**Igf1r*^{-/-} mice led to a small but significant trabecular bone loss (Fig. 2A, B). Thus, sex-specific differences in cancellous bone phenotype and PTH responsiveness in the distal femur were clearly present in 16-week-old control and *OCN**Igf1r*^{-/-} mice infused with PTH over a period of 4 weeks, and those differences paralleled those observed in the responses to serum calcium and ALP.

Connectivity density (Conn. Dens.) was substantially diminished by more than 50% in PTH-infused female control mice compared with vehicle-infused control mice, an effect not found in the female *OCN**Igf1r*^{-/-} mice, whereas male PTH-infused mice did not show a change. A similar pattern was observed for trabecular thickness except that the male *OCN**Igf1r*^{-/-} mice showed a modest but significant reduction in trabecular thickness and mineral content with cPTH consistent with the effect on BV/TV. Trabecular number and separation did not change significantly upon PTH infusion in control and *OCN**Igf1r*^{-/-} mice of either sex, which argues that continuously infused PTH first affects trabecular thickness before reducing the number of trabeculi, thereby maintaining trabecular distribution.

BMD using X-ray attenuation in the volume of interest in cancellous bone was measured. BMD was significantly reduced in the *OCN**Igf1r*^{-/-} mice of both sexes. Like the effects on BV/TV, PTH infusion reduced BMD in the female control mice but had no further effect in the female *OCN**Igf1r*^{-/-} mice, whereas PTH infusion did not alter BMD in the male controls but significantly reduced BMD in the male *OCN**Igf1r*^{-/-} mice (Fig. 2B). The defects in bone mineralization in *OCN**Igf1r*^{-/-} mice are known and have been well documented previously. If voxels below the threshold for mineralized bone were excluded (undermineralized bone and non-bone voxels), these differences were attenuated.

Sex and genotype differences in the effect of PTH infusion on cortical bone

To assess the effects of cPTH on cortical bone, we investigated the midshaft femur region. As in the distal femur, the male bones were bigger with respect to cross-sectional area, but no difference in size was observed between control and knockout mice. However, the *OCN**Igf1r*^{-/-} mice of both sexes had a reduced cortical bone area and cortical thickness (Fig. 2C). In female mice, cPTH reduced cortical thickness in the controls but not in the *OCN**Igf1r*^{-/-} mice, whereas in male mice, only the *OCN**Igf1r*^{-/-} mice showed a reduction

with cPTH (Fig. 2C). The effects in cortical bone were more modest than those found in cancellous bone, and transverse μ CT sections of that region in the PTH-infused groups did not show marked differences in cortical porosity compared with control groups. The results argue that osteocytes and endo- and periosteal lining cells in the cortical bone of control mice have limited responsiveness to the effects of cPTH compared with the cells of trabecular bone at least in this genetic background. Nevertheless, the interaction of sex and genotype in cortical bone is comparable to that of cancellous bone with respect to the effect of cPTH.

Sex and genotype differences in the effect of PTH infusion on bone formation and mineralization in vivo

To further investigate how PTH affects bone remodeling in the *OCN**Igf1r*^{-/-} and control mice, we performed bone histomorphometry to determine BFR and MAR. As shown in Fig. 3, {FIG3} PTH increased BFR (twofold in female and 1.9-fold in male) and MAR (1.8-fold in female, twofold in male) in the control mice of both sexes (Fig. 3B, C). However, the stimulatory effects of cPTH on BFR and MAR were completely blocked in the female *OCN**Igf1r*^{-/-} mice (Fig. 3B, C), whereas the male *OCN**Igf1r*^{-/-} mice continued to show a partial stimulatory response (Fig. 3B, C).

Sex and genotype differences in the effect of PTH infusion on osteoblast differentiation in vitro

To better understand the effects of continuous PTH on female and male osteoblast differentiation and mineralization, we cultured BMSCs from mice, which were either exposed to 4 weeks of vehicle or cPTH treatment in vivo. The number of alkaline phosphatase (ALP⁺) staining colonies was significantly increased upon PTH infusion in female and male control mice (Fig. 4A, C, D). {FIG4} However, BMSC from PTH-infused male control mice had a significantly greater number of ALP⁺ colonies than those from the female mice. The effects of PTH on ALP⁺ colony numbers were abrogated in PTH-infused female *OCN**Igf1r*^{-/-} mice, whereas vehicle-infused female *OCN**Igf1r*^{-/-} mice showed an unchanged number of ALP⁺ colonies compared with female vehicle-infused controls (Fig. 4A, C). Surprisingly, an increase in ALP⁺ colonies was apparent in vehicle-infused male *OCN**Igf1r*^{-/-} mice compared with male controls with a partial further increase after PTH infusion (Fig. 4A, D). As found in vivo, these results indicate that male osteoblasts are not as dependent on the IGF1R for their response to PTH as are the osteoblasts from female mice.

A similar pattern is seen when the ability of the BMSC to mineralize is examined (Fig. 4B–D). BMSCs from vehicle-infused male mice formed 10 times as many mineralized nodules as BMSCs from vehicle-infused female mice (Fig. 4B–D). cPTH further increased the number of mineralized nodules in both sexes, but the increase in absolute numbers was greater in the BMSC from the male mice (Fig. 4B–D). The knockout of *Igf1r* almost completely abrogated the formation of mineralized nodules in BMSC from vehicle-infused female and male mice and blocked the increase in mineralized nodules after cPTH in the female *OCN**Igf1r*^{-/-} mice. However, male *Igf1r* mice responded to the stimulatory effect of cPTH with respect to mineralized nodule formation (Fig. 4B–D).

Stimulation of osteoclastogenesis by cPTH is blocked in *OCN**Igf1r*^{-/-} mice

Compared with the adherent, large, and multinucleated osteoclasts of control mice, the osteoclasts from *OCN**Igf1r*^{-/-} mice were smaller and not well attached to the bone surface (Fig. 5A). {FIG5} To delineate the effects of cPTH on osteoclast formation in mice lacking *Igf1r* in mature osteoblasts and osteocytes, co-cultures of osteoblasts and osteoclasts were examined (Fig. 5B). Osteoblasts from male mice stimulated osteoclastogenesis more effectively than did osteoblasts from female mice. However, both female and male osteoblasts from control mice exposed to continuous PTH for 4 weeks supported osteoclastogenesis more efficiently than osteoblasts from vehicle-infused mice. *Igf1r* deletion in mature osteoblasts and osteocytes appeared to increase the ability of these cells to stimulate osteoclastogenesis, although *Igf1r* deletion rendered the osteoblasts insensitive to further stimulation by PTH infusion with respect to this function. When the response of osteoclast precursors to RANKL/mCSF was studied directly in the absence of osteoblasts, the precursors from the female mice formed twice as many osteoclasts as those from male mice (Fig. 5C), indicating greater sensitivity to RANKL/mCSF. These results are the opposite of those found in the co-culture experiments but are consistent with the greater sensitivity of female mice to the catabolic actions of PTH. As expected, no difference was observed when the osteoclast precursors were obtained from *OCN**Igf1r*^{-/-} mice compared with their normal littermates.

cPTH affects osteoblastic and osteoclastic markers in a sex-specific manner

We then examined the impact of PTH infusion on the expression of genes involved with osteoblast and osteoclast differentiation using quantitative PCR of bone extracts (marrow removed) after the 4-week infusion with vehicle or cPTH (Fig. 6). {FIG6} *Igf1* expression was higher in the bone of male control versus female control mice after vehicle infusion but was markedly reduced in both sexes after cPTH (Fig. 6A). Deleting *Igf1r* from the mature osteoblasts and osteocytes of these mice decreased *Igf1* expression and blocked further changes with cPTH. Alkaline phosphatase (*Alpl*) expression was not affected by PTH in control or *OCN**Igf1r*^{-/-} female mice but was stimulated more than fivefold in the male mice, including the *OCN**Igf1r*^{-/-} male mice (Fig. 6B). Osteocalcin (*Bglap*) expression was stimulated by cPTH in both sexes of control mice and, like *Alpl*, was also increased in the *OCN**Igf1r*^{-/-} male but not female mice (Fig. 6C). cPTH stimulated RANKL (*Tnfs11*) expression more in the bone of female control mice than in male control mice and, like *Alpl* and *Bglap* expression, cPTH also stimulated *Tnfs11* expression in the male but not in female *OCN**Igf1r*^{-/-} mouse (Fig. 6D). On the other hand, osteoprotegerin (*Tnfrs11b*) expression was stimulated more than tenfold by cPTH in male control mice with no increase in female control mice (Fig. 6E). This expression was blunted but still significant in the male *OCN**Igf1r*^{-/-} mice (Fig. 6E). As such, the ratio of *Tnfs11*/*Tnfrs11b* expression was increased by PTH in the female control mice but inhibited in both control and *OCN**Igf1r*^{-/-} male mice (Fig. 6F). Consistent with these results, the expression of RANK (*Tnfrs11a*) was increased significantly only in the female control mice and to a lesser extent in the male *OCN**Igf1r*^{-/-} mice (Fig. 6G). These results support the in vivo data that cPTH is more catabolic in female mice than in male mice and more dependent on IGF1 signaling in female mice.

Discussion

That iPTH is anabolic and cPTH is catabolic has become dogma. Indeed, at the start of this project, we proceeded under that expectation, asking whether the catabolic actions of PTH were dependent on IGF1 signaling like the anabolic actions. However, there are hints in the literature that sex would influence these results.^(2,33,34) Moreover, in earlier studies with daily injections of PTH over a two-week course, we⁽³⁵⁾ found that male mice had a greater response with respect to periosteal bone formation and a greater response with respect to increased *Igf1* expression. Thus, it was not totally unexpected that when examining the impact of *Igf1r* deletion on the skeletal response to cPTH, sex would influence the results and add a caveat to the dogma that cPTH is only catabolic.

As suggested by the clinical studies and earlier reports on sex differences in PTH responsiveness in bone, cPTH was substantially more catabolic in the female control mice than in the male control mice. This was manifested by a loss in BV/TV, connectivity density, and trabecular thickness in the cancellous bone of the distal femur in control female mice but not in control male mice after cPTH. Similarly, cortical thickness of the femur diaphysis was reduced by cPTH in the female control mice but not in the male control mice.

We then looked at bone formation and resorption to determine where the differences in responses to PTH between males and females of the different genotypes might lie. MAR and BFR were stimulated by cPTH in both male and female control mice. However, BMSC from male mice in vitro showed a significantly greater response to cPTH given in vivo with respect to numbers of ALP⁺ colonies and mineralized nodules, markers of an anabolic response. The osteoblasts from both sexes of control mice given cPTH in vivo demonstrated increased ability to induce osteoclast formation in vitro. We anticipated that cPTH might have a greater stimulation of osteoclastogenesis in female mice, but that was not found in these in vitro co-culture experiments. On the other hand, the osteoclast precursors from female mice were twice as sensitive to exogenous RANKL/mCSF with respect to osteoclast formation that might at least partially explain the increased sensitivity of female mice to the catabolic actions of PTH. Moreover, the analysis of gene expression in the intact bone supported this conclusion as discussed below.

Differences between control male and female mice with respect to the response of gene expression in intact bone to cPTH are quite revealing with respect to why cPTH has a much greater catabolic effect on female mice. Stimulation of *Alpl* expression by cPTH was much greater in control male mice than in control female mice, although the stimulation of *Bglap* expression was equivalent. Moreover, cPTH-stimulated *Tnfs11* (*Rankl*) expression was much greater in control female mice than in control male mice, and the opposite was true for *Tnfrs11b* (*osteoprotegerin*) expression. Thus, the higher ratio of *Tnfs11/Tnfrs11b* expression in the female control mice strongly favored increased osteoclastogenesis and bone resorption in response to cPTH in these mice. Although *Igf1* expression basally was higher in the male control mice and cPTH increased the circulating concentrations of IGF1 only in the males, cPTH suppressed *Igf1* expression in the bone of both male and female mice, so this was not an obvious factor in the differential response of male and female bone

to cPTH. This suppression of *Igf1* expression by cPTH in bone confirms results of others⁽²¹⁾ and differs from the increase in *Igf1* expression by iPTH.^(14,35,36)

We are not the first to report such sex differences in bone, however. In a recent publication, Zanotti and colleagues⁽³⁷⁾ noted in several mouse strains including FVB that the BMSC from female mice had lower *Alpl* and *Bglap* expression with decreased alkaline phosphatase activity and fewer mineralized nodules, findings we confirmed in this study. Moreover, calvarial cells from female C57BL/6 mice expressed more *Tnfs11* and less *Tnfrs11b* than cells from males, again consistent with our results. The response to PTH was not examined in that study.

However, the initial impetus for this study was to determine whether deleting *Igf1r* from mature osteoblasts and osteocytes would block the catabolic actions of cPTH as we had previously shown for the anabolic actions of iPTH.⁽²⁶⁾ First, the bones of the *OCN**Igf1r*^{-/-} mice were comparable in size to their wild-type littermates of the same sex, although as expected bone volume and thus BV/TV was lower in both sexes of the *OCN**Igf1r*^{-/-} mice. In the female *OCN**Igf1r*^{-/-} mice, cPTH had no further impact on BV/TV, thus demonstrating that IGF1 signaling was required for the catabolic actions. This lack of response to cPTH in the female *OCN**Igf1r*^{-/-} mouse was true for both cancellous and cortical bone. Moreover, cPTH failed to stimulate BFR in the female *OCN**Igf1r*^{-/-} mice, unlike their littermate controls. The big surprise was that the male *OCN**Igf1r*^{-/-} actually showed a small but significant reduction in BV/TV, trabecular thickness, mineral content, and cortical bone area and thickness after cPTH even though the control males did not. The BMSC cultures confirmed this differential response of male and female *OCN**Igf1r*^{-/-} mice in that BMSC from male *OCN**Igf1r*^{-/-} mice after cPTH showed a response with respect to increased alkaline phosphatase activity and mineralized nodule formation, whereas the BMSC from female *OCN**Igf1r*^{-/-} mice did not. Although we could not demonstrate a differential response to cPTH with respect to osteoblast stimulation of osteoclast formation in vitro between male and female *OCN**Igf1r*^{-/-} mice (neither responded to cPTH in this regard, although basal levels of osteoblast-induced osteoclastogenesis were higher in the *OCN**Igf1r*^{-/-}), the expression of genes relevant to osteoblast and osteoclast differentiation in bone after cPTH was very different between male and female *OCN**Igf1r*^{-/-} mice. Female *OCN**Igf1r*^{-/-} mice showed no significant increase in *Igf1*, *Alpl*, *Bglap*, *Tnfs11*, or *Tnfrs11b* expression after cPTH, whereas the response of male *OCN**Igf1r*^{-/-} mice to cPTH with respect to the expression of *Alpl*, *Bglap*, *Tnfs11*, and *Tnfrs11a* was equivalent to their littermate controls.

At this point, we do not have a clear understanding of why sex differences are found in the response of bone to PTH, why there are sex differences in the role of IGF1 signaling in mediating the actions of PTH on bone, and why these differences persist in vitro. One obvious difference between males and females is sex hormones. Loss of estrogen has been invoked as one explanation for the higher prevalence of primary hyperparathyroidism in the postmenopausal female compared with comparably aged males, which may better maintain their testosterone concentrations as they age. Lee and colleagues⁽³⁸⁾ showed that both testosterone and estrogen withdrawal increased the skeletal response to a 24-hour infusion to PTH, although estrogen withdrawal seemed to have a greater impact than testosterone withdrawal. Other studies have shown that the estrogen receptor alpha is required for IGF1R

activation by mechanical load in osteoblasts.⁽³⁹⁾ However, the mice in this study were not androgen or estrogen deprived and quite fertile, and differences in hormones would not readily explain the persistence of the sex differences in vitro. Thus, an understanding of the sex differences revealed in this study with respect to the skeletal actions of PTH and the role of IGF1 signaling in mediating the skeletal actions of PTH remains for future investigation, but points to the need to consider both sexes in studies of this nature. That said, the prime goal of this study to determine whether IGF1 signaling was required for the catabolic actions of PTH on bone has been accomplished. We found it to be required for female mice but less so for male mice.

Supplementary Material

Refer to Web version on PubMed Central for supplementary material.

Acknowledgments

We thank Dr Thomas Clemens for providing us with *OCN^{tgflr}^{-/-}* mice and Wenhan Chang for overseeing the bone core unit, which performed μ CT scans and embedded the bones. This work was supported by NIH grants RO1 AR055924 (DDB), by the Department of Veteran Affairs Research Enhancement Award Program in Bone Disease RO1DK054793 (DDB), as well as Merit Review and the VA Program Project Reward (DDB) and by Janggen Pöhn and Novartis research fellowships (MB).

References

1. Lundgren E, Rastad J, Thruvbjerg E, Akerstrom G, Ljunghall S. Population-based screening for primary hyperparathyroidism with serum calcium and parathyroid hormone values in menopausal women. *Surgery*. 1997;121(3):287–94. [PubMed: 9092129]
2. Wermers RA, Khosla S, Atkinson EJ, et al. Incidence of primary hyperparathyroidism in Rochester, Minnesota, 1993–2001: an update on the changing epidemiology of the disease. *J Bone Miner Res*. 2006;21(1):171–7. [PubMed: 16355286]
3. Shinoda Y, Kawaguchi H, Higashikawa A, et al. Mechanisms underlying catabolic and anabolic functions of parathyroid hormone on bone by combination of culture systems of mouse cells. *J Cell Biochem*. 2010;109(4):755–63. [PubMed: 20058231]
4. Datta NS, Abou-Samra AB. PTH and PTHrP signaling in osteoblasts. *Cell Signal*. 2009;21(8):1245–54. [PubMed: 19249350]
5. Rhee Y, Lee EY, Lezcano V, et al. Resorption controls bone anabolism driven by parathyroid hormone (PTH) receptor signaling in osteocytes. *J Biol Chem*. 2013;288(41):29809–20. [PubMed: 23963454]
6. Neer RM, Arnaud CD, Zanchetta JR, et al. Effect of parathyroid hormone (1–34) on fractures and bone mineral density in postmenopausal women with osteoporosis. *N Engl J Med*. 2001;344(19):1434–41. [PubMed: 11346808]
7. Black DM, Greenspan SL, Ensrud KE, et al. The effects of parathyroid hormone and alendronate alone or in combination in postmenopausal osteoporosis. *N Engl J Med*. 2003;349(13):1207–15. [PubMed: 14500804]
8. Finkelstein JS, Hayes A, Hunzelman JL, Wyland JJ, Lee H, Neer RM. The effects of parathyroid hormone, alendronate, or both in men with osteoporosis. *N Engl J Med*. 2003;349(13):1216–26. [PubMed: 14500805]
9. Lindsay R, Zhou H, Cosman F, Nieves J, Dempster DW, Hodsmann AB. Effects of a one-month treatment with PTH(1–34) on bone formation on cancellous, endocortical, and periosteal surfaces of the human ilium. *J Bone Miner Res*. 2007;22(4):495–502. [PubMed: 17227219]
10. Nishida S, Yamaguchi A, Tanizawa T, et al. Increased bone formation by intermittent parathyroid hormone administration is due to the stimulation of proliferation and differentiation of osteoprogenitor cells in bone marrow. *Bone*. 1994;15(6):717–23. [PubMed: 7873302]

11. Bellido T, Ali AA, Gubrij I, et al. Chronic elevation of parathyroid hormone in mice reduces expression of sclerostin by osteocytes: a novel mechanism for hormonal control of osteoblastogenesis. *Endocrinology*. 2005;146(11):4577–83. [PubMed: 16081646]
12. Canalis E, Centrella M, Burch W, McCarthy TL. Insulin-like growth factor I mediates selective anabolic effects of parathyroid hormone in bone cultures. *J Clin Invest*. 1989;83(1):60–5. [PubMed: 2910920]
13. Pfeilschifter J, Laukhuf F, Muller-Beckmann B, Blum WF, Pfister T, Ziegler R. Parathyroid hormone increases the concentration of insulin-like growth factor-I and transforming growth factor beta 1 in rat bone. *J Clin Invest*. 1995;96(2):767–74. [PubMed: 7635970]
14. Watson P, Lazowski D, Han V, Fraher L, Steer B, Hodsman A. Parathyroid hormone restores bone mass and enhances osteoblast insulin-like growth factor I gene expression in ovariectomized rats. *Bone*. 1995;16(3):357–65. [PubMed: 7786639]
15. Jilka RL, Weinstein RS, Bellido T, Roberson P, Parfitt AM, Manolagas SC. Increased bone formation by prevention of osteoblast apoptosis with parathyroid hormone. *J Clin Invest*. 1999;104:439–46. [PubMed: 10449436]
16. Dobnig H, Turner RT. Evidence that intermittent treatment with parathyroid hormone increases bone formation in adult rats by activation of bone lining cells. *Endocrinology*. 1995;136(8):3632–8. [PubMed: 7628403]
17. Ma YL, Cain RL, Halladay DL, et al. Catabolic effects of continuous human PTH (1–38) in vivo is associated with sustained stimulation of RANKL and inhibition of osteoprotegerin and gene-associated bone formation. *Endocrinology*. 2001;142(9):4047–54. [PubMed: 11517184]
18. Frolik CA, Black EC, Cain RL, et al. Anabolic and catabolic bone effects of human parathyroid hormone (1–34) are predicted by duration of hormone exposure. *Bone*. 2003;33(3):372–9. [PubMed: 13678779]
19. O'Brien CA, Plotkin LI, Galli C, et al. Control of bone mass and remodeling by PTH receptor signaling in osteocytes. *PLoS ONE*. 2008;3(8):e2942. [PubMed: 18698360]
20. Huang JC, Sakata T, Pflieger LL, et al. PTH differentially regulates expression of RANKL and OPG. *J Bone Miner Res*. 2004;19(2):235–44. [PubMed: 14969393]
21. Locklin RM, Khosla S, Turner RT, Riggs BL. Mediators of the biphasic responses of bone to intermittent and continuously administered parathyroid hormone. *J Cell Biochem*. 2003;89(1):180–90. [PubMed: 12682918]
22. Kostenuik PJ, Harris J, Halloran BP, Turner RT, Morey-Holton ER, Bikle DD. Skeletal unloading causes resistance of osteoprogenitor cells to parathyroid hormone and to insulin-like growth factor-I. *J Bone Miner Res*. 1999;14(1):21–31.
23. Wang Y, Nishida S, Elalieh HZ, Long RK, Halloran BP, Bikle DD. Role of IGF-I signaling in regulating osteoclastogenesis. *J Bone Miner Res*. 2006;21(9):1350–8. [PubMed: 16939393]
24. Bikle D, Majumdar S, Laib A, et al. The skeletal structure of insulin-like growth factor I-deficient mice. *J Bone Miner Res*. 2001;16(12): 2320–29. [PubMed: 11760848]
25. Zhang M, Xuan S, Bouxsein ML, et al. Osteoblast-specific knockout of the insulin-like growth factor (IGF) receptor gene reveals an essential role of IGF signaling in bone matrix mineralization. *J Biol Chem*. 2002;277(46):44005–12. [PubMed: 12215457]
26. Wang Y, Nishida S, Boudignon BM, et al. IGF-I receptor is required for the anabolic actions of parathyroid hormone on bone. *J Bone Miner Res*. 2007;22(9):1329–37. [PubMed: 17539737]
27. Cheng Z, Liang N, Chen TH, et al. Sex and age modify biochemical and skeletal manifestations of chronic hyperparathyroidism by altering target organ responses to Ca²⁺ and parathyroid hormone in mice. *J Bone Miner Res*. 2013;28(5):1087–1100. [PubMed: 23239173]
28. Wang Y, Clemens TL, Bikle DD, Chang W. Chondrocyte-specific knockout of the IGF-IR impedes chondrocyte growth, survival, and differentiation. *J Bone Min Res*. 2006;21:S50.
29. Bouxsein ML, Boyd SK, Christiansen BA, Guldberg RE, Jepsen KJ, Muller R. Guidelines for assessment of bone microstructure in rodents using micro-computed tomography. *J Bone Miner Res*. 2010;25(7):1468–86. [PubMed: 20533309]
30. Dempster DW, Compston JE, Drezner MK, et al. Standardized nomenclature update of the report of the ASBMR Histomorphometry Nomenclature Committee. *J Bone Miner Res* 2012; 28(1): 2–17.

31. Wang Y, Menendez A, Fong C, Elalieh HZ, Chang W, Bikle DD. Ephrin B2/EphB4 mediates the actions of IGF-I signaling in regulating endochondral bone formation. *J Bone Miner Res* 2014;29(8): 1900–13. [PubMed: 24677183]
32. Mosekilde L Primary hyperparathyroidism and the skeleton. *Clin Endocrinol (Oxf)*. 2008;69(1):1–19. [PubMed: 18167138]
33. Rico H, Revilla M, Arribas I, Villa LF, Alvarez de Buergo. Total and regional bone mineral content in primary hyperparathyroidism: sex differences. *Miner Electrolyte Metab*. 1994;20(3):112–6. [PubMed: 7815998]
34. Shah VN, Bhadada SK, Bhansali A, Behera A, Mittal BR, Bhavin V. Influence of age and gender on presentation of symptomatic primary hyperparathyroidism. *J Postgrad Med*. 2012;58(2):107–11. [PubMed: 22718053]
35. Wang Y, Sakata T, Elalieh HZ, et al. Gender differences in the response of CD-1 mouse bone to parathyroid hormone: potential role of IGF-I. *J Endocrinol*. 2006;189(2):279–87. [PubMed: 16648295]
36. Pfeilschifter J, Laukhuf F, Muller-Beckmann B, Blum WF, Pfister T, Ziegler R. Parathyroid hormone increases the concentration of insulin-like growth factor-1 and transforming growth factor beta 1 in rat bone. *J Clin Invest*. 1995;96:767–74. [PubMed: 7635970]
37. Zanotti S, Kalajzic I, Aguila HL, Canalis E. Sex and genetic factors determine osteoblastic differentiation potential of murine bone marrow stromal cells. *PLoS ONE*. 2014;9(1):e86757. [PubMed: 24489784]
38. Lee H, Finkelstein JS, Miller M, Comeaux SJ, Cohen RI, Leder BZ. Effects of selective testosterone and estradiol withdrawal on skeletal sensitivity to parathyroid hormone in men. *J Clin Endocrinol Metab*. 2006;91(3):1069–75. [PubMed: 16352679]
39. Sunters A, Armstrong VJ, Zaman G, et al. Mechano-transduction in osteoblastic cells involves strain-regulated estrogen receptor alpha-mediated control of insulin-like growth factor (IGF) I receptor sensitivity to Ambient IGF, leading to phosphatidylinositol 3-kinase/AKT-dependent Wnt/LRP5 receptor-independent activation of beta-catenin signaling. *J Biol Chem*. 2010;285(12):8743–58. [PubMed: 20042609]

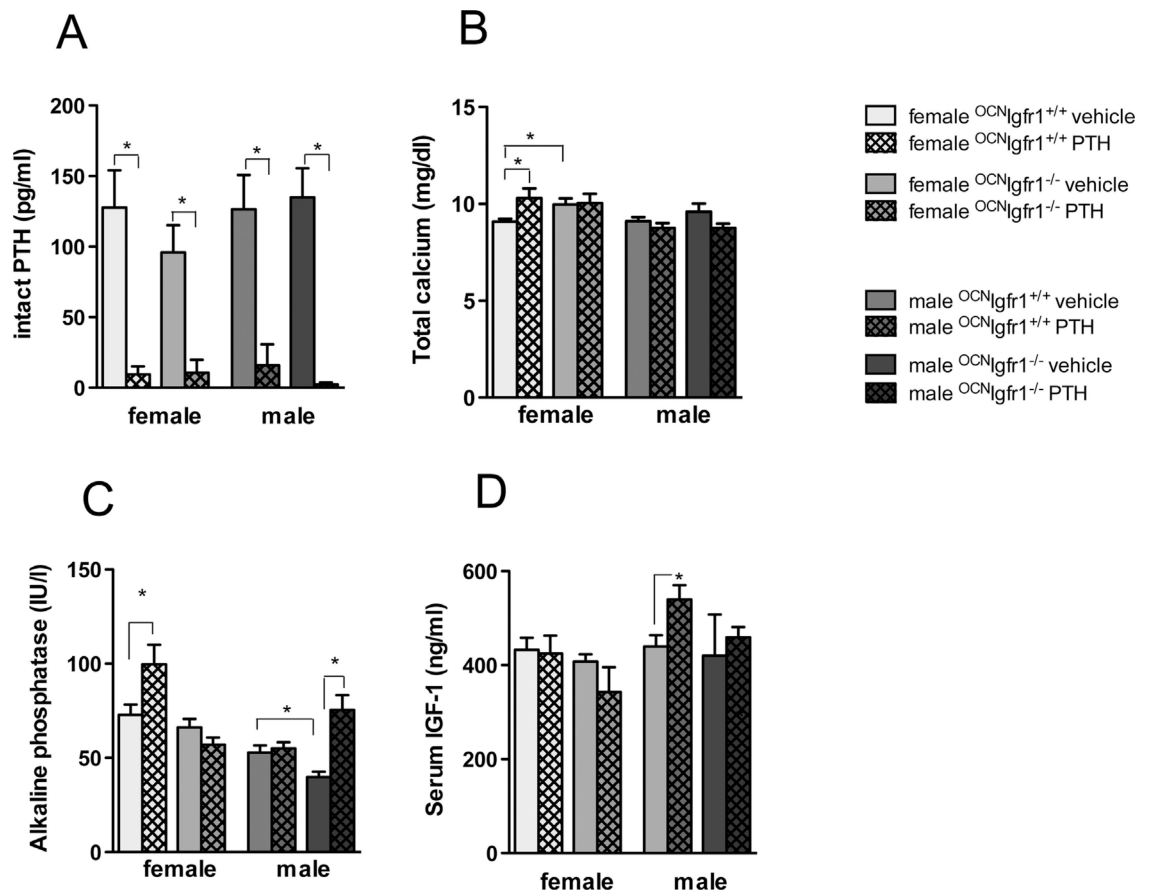


Fig. 1. Suppressed endogenous PTH concentrations and sex-specific impact on calcium, alkaline phosphatase, and IGF-1 concentrations in continuously PTH-infused *OCN**Igfr1*^{-/-} mice. Serum intact PTH (A), total calcium (B), alkaline phosphatase (C), and IGF-1 (D) concentrations in continuously PTH- and vehicle-infused *OCN**Igfr1*^{-/-} and control mice ($n=8-12$). The error bars enclose mean \pm SE; * $p < 0.05$.

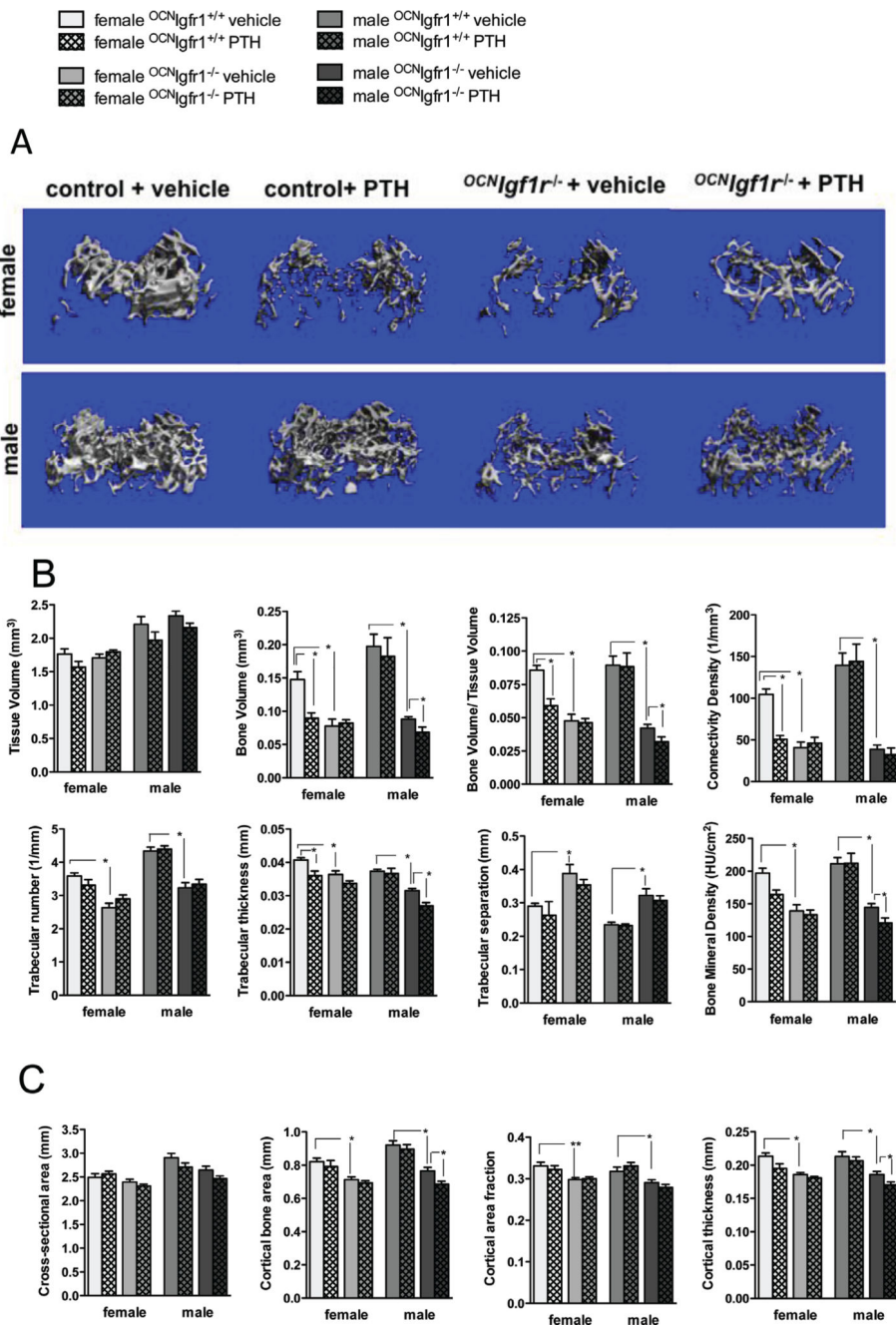


Fig. 2. Net catabolic effects of continuous PTH infusion in female control mice were blocked in female $OCN1gfr1^{-/-}$ mice; the response in male mice differed. (A) Representative micro-CT 3D reconstructions of the secondary spongiosa of the distal femoral metaphysis in female and male continuously PTH- and vehicle-infused $OCN1gfr1^{-/-}$ and control mice. (B) Quantitative analysis of trabecular bone in distal femurs from 16-week-old continuously PTH- and vehicle-infused $OCN1gfr1^{-/-}$ and control mice with micro-CT ($n=8-12$). Tissue volume (mm^3), bone volume (mm^3), bone volume/tissue volume, connectivity density ($1/mm^3$), trabecular number ($1/mm$), trabecular thickness (mm), trabecular separation (mm),

and mineral content (HU/cm²) are shown. (C) Quantitative analysis of cortical bone in midshaft femurs from 16-week-old continuously PTH- and vehicle-infused *OCN*^{0/0}*Igf1r*^{-/-} and control mice with micro-CT (*n*=8–12). Cross-sectional area (mm²), cortical bone area (mm²), cortical area fraction, and cortical thickness (mm) are shown. Data are shown as mean ± SE; **p*< 0.05.

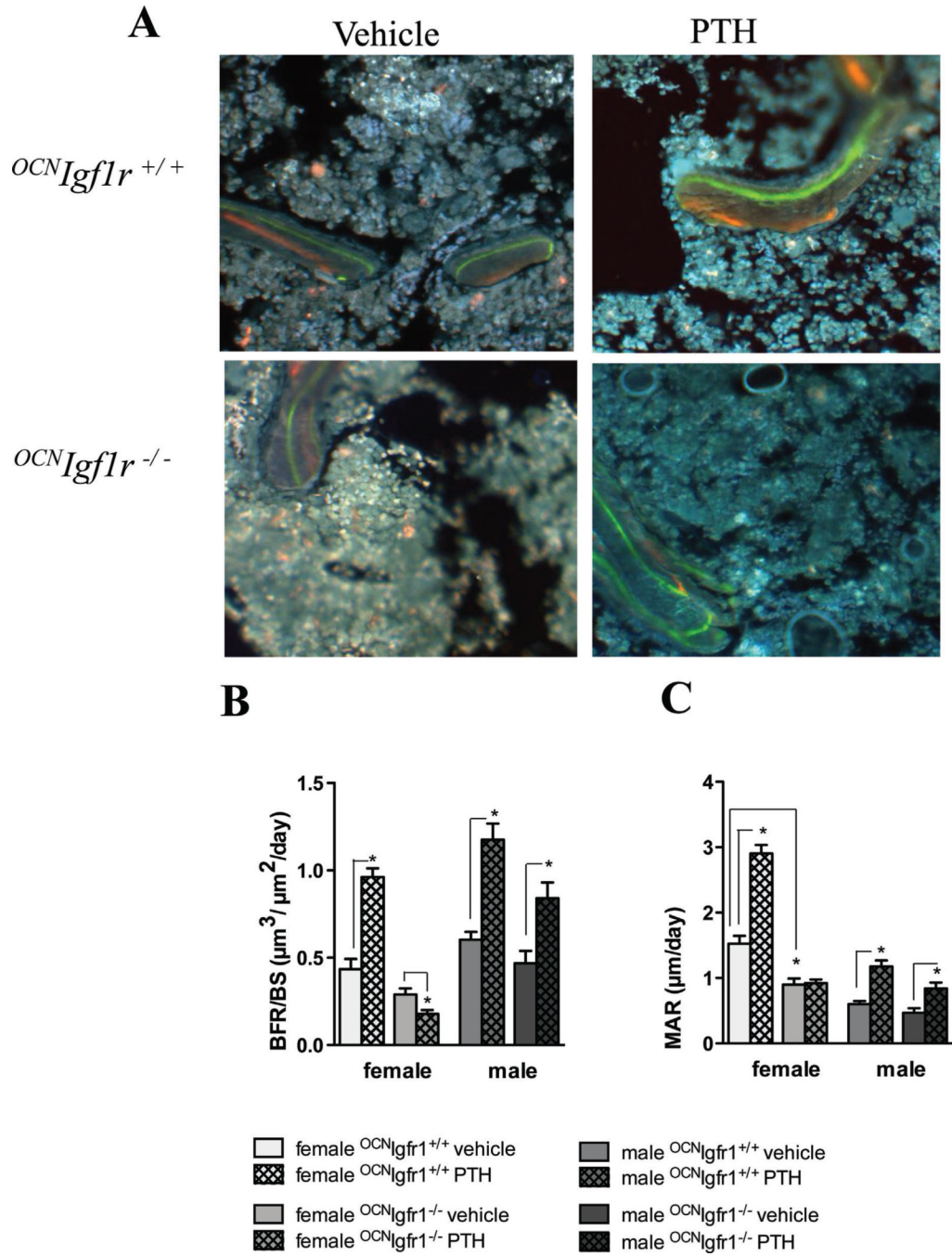


Fig. 3. Stimulatory effects of continuous PTH on bone formation and mineral apposition rate are blocked in female but not in male *OCN**Igfr1*^{-/-} mice. (A) Representative fluorescent double-labeled sections of trabecular bone in PTH- and vehicle-infused *OCN**Igfr1*^{-/-} and control mice are shown. (B) Quantitative analysis of bone formation rate/bone surface ($\mu\text{m}^3/\mu\text{m}^2/\text{d}$) in continuous PTH- and vehicle-infused female and male *OCN**Igfr1*^{-/-} and control mice ($n=4$). Data are shown as mean \pm SE; * $p < 0.05$. (C) Quantitative analysis of mineral

apposition rate (mm/d) in continuous PTH- and vehicle-infused female and male *OCN*^{IGF1R}^{-/-} and control mice (*n*=4). Data are shown as mean ± SE; **p* < 0.05.

Author Manuscript

Author Manuscript

Author Manuscript

Author Manuscript

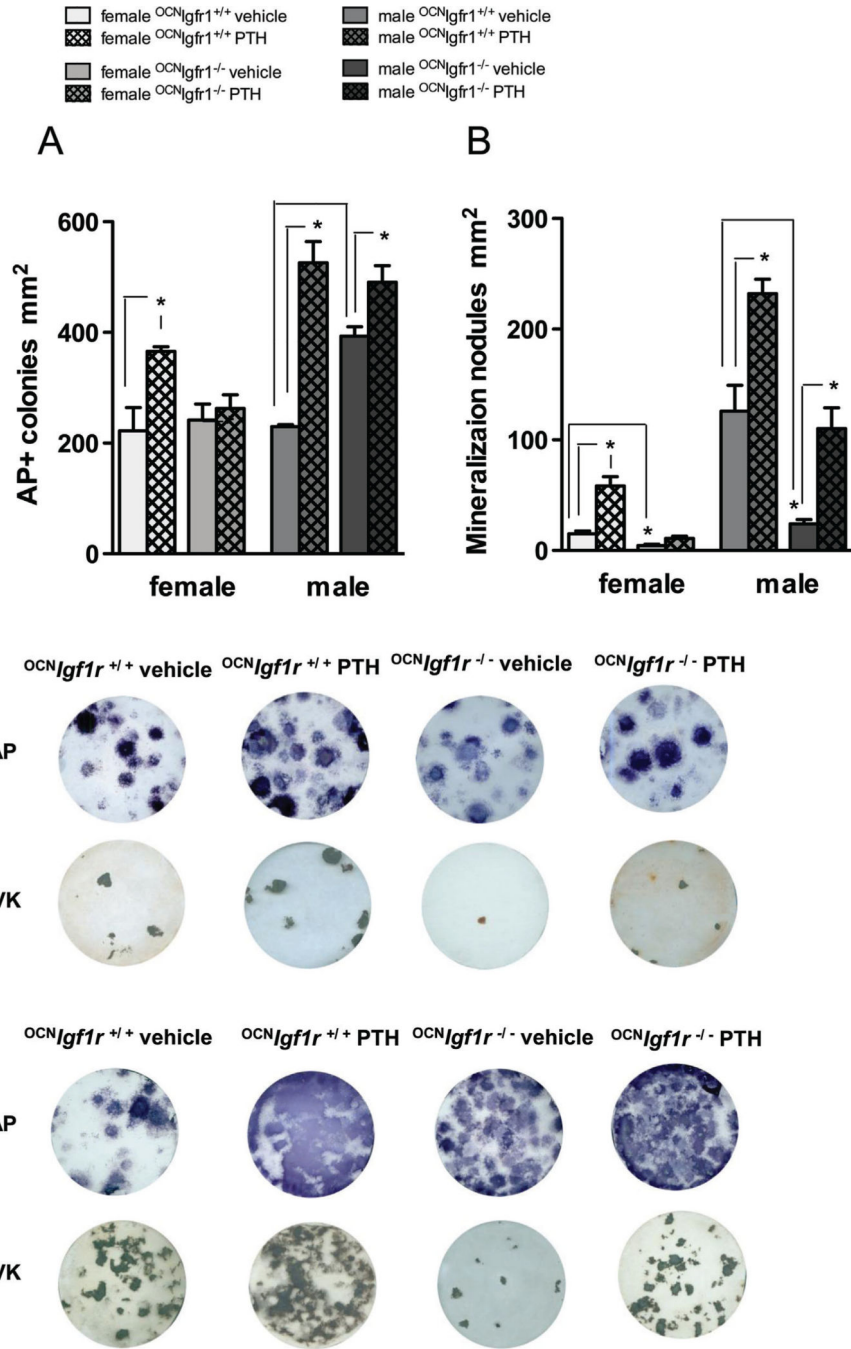


Fig. 4. Osteoblast stimulatory effects of continuous PTH were less robust when assessed in female control bone marrow stromal cell (BMSC) cultures and abrogated in those from female *OCN Igf1r*^{-/-} mice. (A) Quantitative analysis of alkaline phosphatase (ALP)⁺ colony-forming units (CFUs) at day 14 of BMSCs after 4-week in vivo exposure to continuous PTH or vehicle in *OCN Igf1r*^{-/-} and control mice (*n*=8–12). (B) Quantitative analysis of mineralization nodules at day 21 of bone marrow stromal cell cultures after 4-week in vivo exposure to continuous PTH or vehicle in *OCN Igf1r*^{-/-} and control mice (*n*=8–12). Data are

shown as mean \pm SE; * $p < 0.05$. (C) A representative bone marrow stromal cell culture image is displayed for alkaline phosphatase staining at 14 days and mineralization nodules at 21 days for continuously PTH- and vehicle-infused female and male *OCN*^{*Igf1r*^{-/-}} and control mice ($n=8-12$).

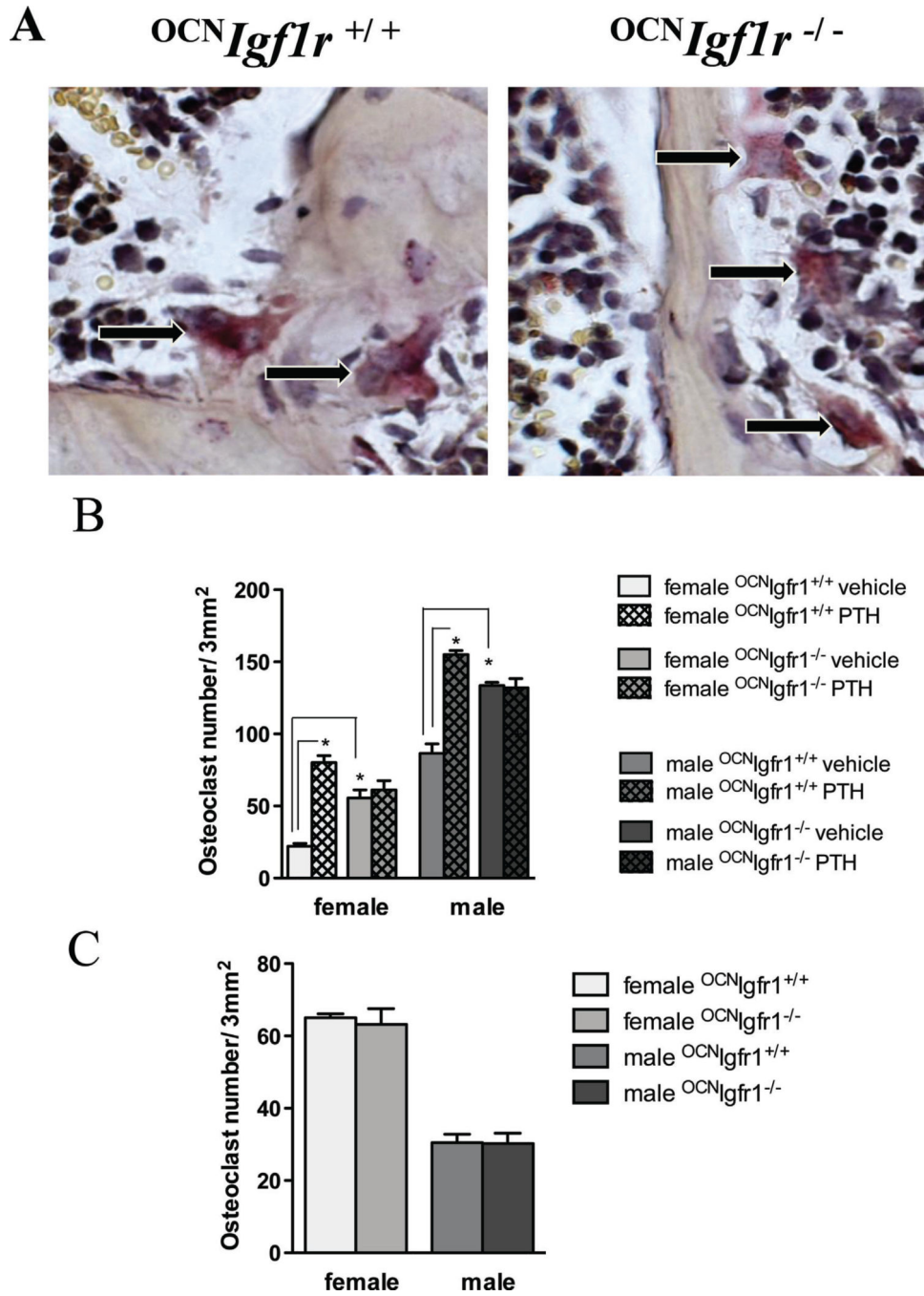


Fig. 5. Knockout of *Igfr1* affects osteoclast maturation. (A) Representative sections of TRAP-stained osteoclasts on trabecular bone in control and *OCN**Igfr1*^{-/-} mice. Magnification ×40. (B) Quantitative analysis of osteoclast counts after 7 days of osteoclast/osteoblast co-culture. The control and *OCN**Igfr1*^{-/-} osteoblasts were either exposed to 4 weeks of vehicle or continuous PTH infusion in vivo before harvest. Osteoclast precursors from bone marrow were taken from a separate group of 16-week-old control mice (*n*=4–6). Data are shown as mean ± SE; **p* < 0.05. (C) Osteoclast formation after RANKL/mCSF administration to

cultures of osteoclast precursors from male and female control and *OCN**Igfl1*^{-/-} mice (*n*=4 per group). The data are expressed as mean ± SE; **p*< 0.05.

Author Manuscript

Author Manuscript

Author Manuscript

Author Manuscript

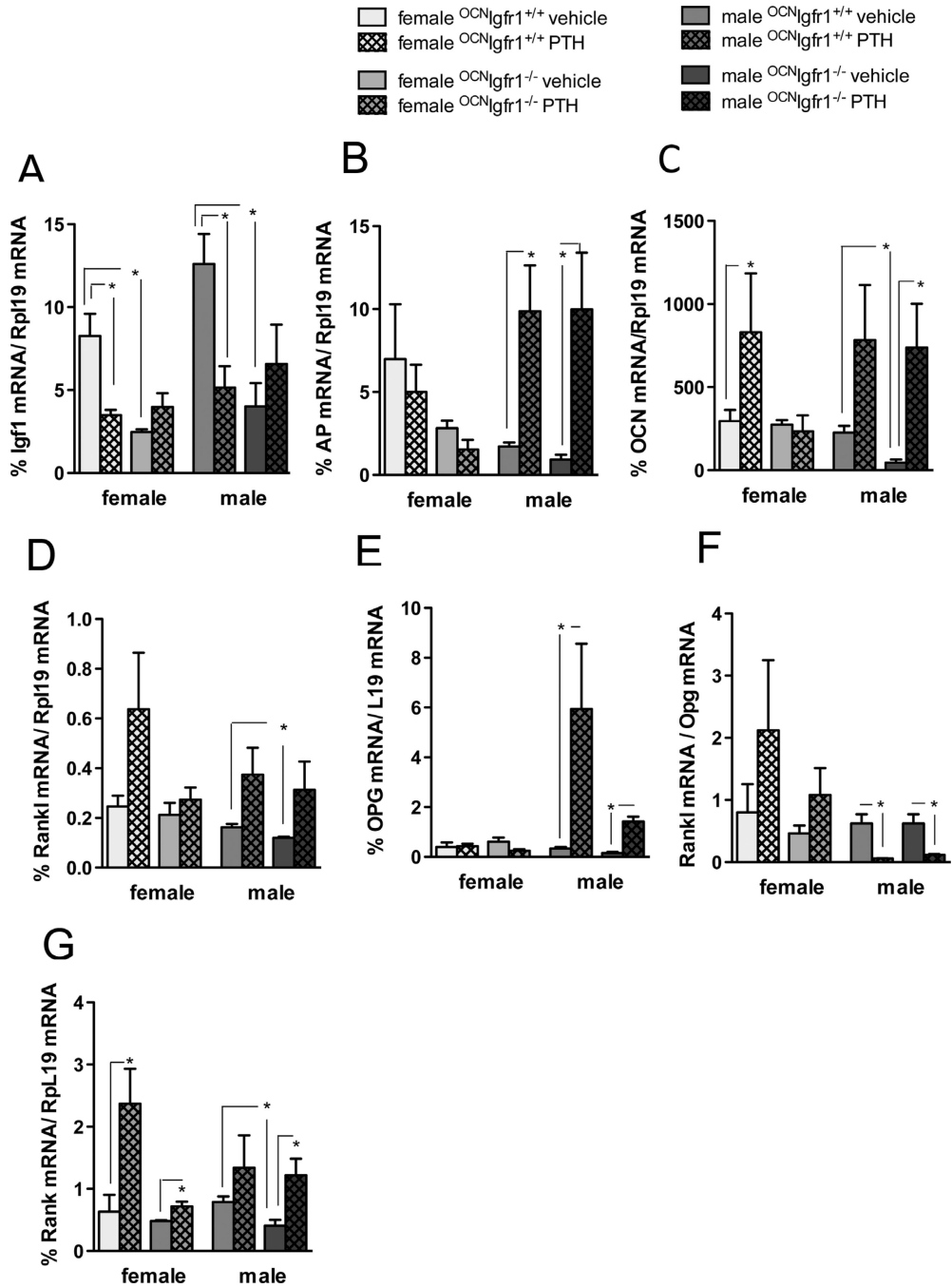


Fig. 6. Continuous PTH affects osteoblastic and osteoclastic mRNA markers in a sex-specific manner. (A) Igf-1 mRNA bone expression in diaphysis of long bones (femur and tibia) of 16-week-old continuously PTH- and vehicle-infused *OCN**Igfr1*^{-/-} and control mice. (B) Alkaline phosphatase (ALP) mRNA bone expression in diaphysis of long bones (femur and tibia) of 16-week-old continuously PTH- and vehicle-infused *OCN**Igfr1*^{-/-} and control mice. (C) Osteocalcin (OCN)mRNA bone expression in diaphysis of long bones (femur and tibia) of 16-week-old continuously PTH- and vehicle-infused *OCN**Igfr1*^{-/-} and control mice. (D)

Receptor activator of NF- κ B ligand (RANKL) mRNA bone expression in diaphysis of long bones (femur and tibia) of 16-week-old continuously PTH- and vehicle-infused $^{OCN}Igf1r^{-/-}$ and control mice. (E) Osteoprotegerin (OPG) mRNA bone expression in diaphysis of long bones (femur and tibia) of 16-week-old continuously PTH- and vehicle-infused $^{OCN}Igf1r^{-/-}$ and control mice. (F) RANKL/OPG mRNA ratio bone expression in diaphysis of long bones (femur and tibia) of 16-week-old continuously PTH- and vehicle-infused $^{OCN}Igf1r^{-/-}$ and control mice. (G) RANK mRNA bone expression in diaphysis of long bones (femur and tibia) of 16-week-old continuously PTH- and vehicle-infused $^{OCN}Igf1r^{-/-}$ and control mice ($n=8-12$). Data are shown as mean \pm SE; * $p < 0.05$.